

# Effect of Process Parameters on Mechanical Properties of Solidified PLA Parts Fabricated by 3D Printing Process



Jagdish Khatwani and Vineet Srivastava

**Abstract** In rapid prototyping (RP), 3D printing is growing fast due to its ability to build different complex geometrical shapes and structures in least possible time. The mechanical behavior of 3D printed parts depends on the interaction of different process parameters and the raw material properties. In this work, the effect of process parameters, namely, nozzle diameter, layer thickness, and part bed temperature, has been studied on mechanical properties like tensile strength and flexural strength in 3D printing process. Material used in the study is solidified polylactic acid (PLA). It was observed that tensile strength and flexural strength increased with increase in part bed temperature. It was further observed that tensile strength decreased with increase with layer thickness whereas flexural strength increased. With respect to nozzle diameter, it was observed that tensile strength increased while flexural strength initially decreased and then increased with increase in nozzle diameter. SEM analysis has been done to evaluate the mechanism of failure of the parts.

**Keywords** 3D printing · Nozzle diameter · Layer thickness · Part bed temperature  
Tensile strength · Flexural strength

## 1 Introduction

Rapid prototyping (RP) technology provides important tools to fabricate geometrically complex functional parts. Compatibility of these RP technologies with computer-aided design (CAD) makes part fabrication faster. Least possible cycle time of design and fabrication is achieved through RP. On the basis of limits on the

---

J. Khatwani · V. Srivastava (✉)  
Department of Mechanical Engineering, Thapar Institute of Engineering & Technology,  
Patiala 147004, Punjab, India  
e-mail: vineet.srivastava@thapar.edu

J. Khatwani  
e-mail: jkhatwani33@gmail.com

type and properties of the material that can be fabricated, many commercial RP systems are available nowadays in the market [1].

Fused Filament modelling (FFM) is one of the most popular 3D printing techniques based on Fused Deposition Modelling (FDM) process. FFM prints a three-dimensional object by depositing a continuous and constant flow of melted work material, which is carefully arranged into layer by layer, starting from the bottom up.

In past, there have been many attempts made to analyze the effect of different process parameters on the mechanical properties of the parts produced through different RP systems. A study made by Ahn et al. [2] showed that air gap and raster orientation affect tensile strength greatly. In FDM parts made with a negative air gap or overlap between roads, the typical tensile strength ranged between 65 and 72% and compressive strength ranged from 80 to 90% of the strength of injection moulded ABS respectively. Karalekas and Antoniou [3] showed that nonwoven fiber mats could improve the mechanical properties of specimens built using the stereolithography and vacuum casting techniques. This study showed that desirable increases in the elastic modulus and the mechanical strength are feasible providing that the reinforcement can be consolidated to the polymer material used. Ang et al. [4] investigated the mechanical properties and porosity relationships in fused deposition modelling. Air gap, Raster width, Build orientation, build lay down pattern, build layer were taken as process parameters. Compressive modulus of the part was only affected by two main parameters—air gap and raster width. Results shows that an increasing air gap caused a mean decrease in the compressive modulus and increasing raster width increase the compressive modulus. Jain et al. [5] used SLS machine and polyamide powder (PA 2200) as material and layer thickness, hatch spacing and scan speed as processing parameters. Parts were fabricated for different ranges of delay time and testing to see the variability in tensile strength. Study showed that if delay time is above or below an optimum value of delay time range, it will result in lower tensile strength. Bagisk et al. [6] pointed out that tensile and compression strengths are influenced by the orientation and the structure of the ABS manufactured parts in FDM. Percoco et al. [7] concluded that compressive strength is increased by 2–4%, when FDM prototypes treated with a solution of 90% dimethylketone and 10% water with raster angle and raster width is taken as process parameters. Croccolo et al. [8] concluded that greater contour will increase stiffness and strength but it will also increase the brittle behavior of the part fabricated by ABS. Theoretical model was developed between responses and parameters successfully.

Tymrak et al. [9] investigated the mechanical properties of ABS and PLA components made using various desktop open-source RepRap three-dimensional printers using build orientation and layer thickness as process parameters. The results showed that the average tensile strength and average elastic modulus of RepRap printed parts for PLA is higher than ABS parts. Afrose et al. [10] investigated the fatigue properties of FDM processed PLA standard tensile parts. These were based on ASTM D638 standard and were cyclically tested at 80, 70, 60, and 50% nominal values of the ultimate tensile stress. Study showed that parts in

*X* build orientation exhibit higher tensile stress, compared to those built in *Y* and 45° orientations. But under tensile cyclic loading condition, the parts in 45° build orientation show higher fatigue life than the parts in *X* and *Y* build orientations for the same percentage of applied static loads. Roberson et al. [11] investigated the effect of stress concentrator fabrication on 3D printed parts using ABS, PC, PC-ABS, and Ultem 9085 as material. Izod impact testing showed that samples printed on the *XY* plane at 45° were shown to have the greatest resistance to impact and samples printed vertically in the *ZXY* orientation had the lowest resistance to impact. Only samples printed from Ultem 9085 experienced a significant difference in impact strength when comparing stress concentrator fabrication method of specimens by printing and milling to develop stress concentrator.

From literature survey, it has been observed that maximum work regarding part strength is concerned on FDM, SL and SLS technologies. In 3D printing, one of the most widely used material is PolyLactic Acid (PLA), which has gained wide popularity due to its light weight and ready availability. PLA is being used for form and fit analysis and as casings for small equipments. It has also been observed that the analysis of strength of parts fabricated through Solidified PLA has not been done before. Therefore an attempt is being made to correlate the tensile strength and flexural strength of solidified PLA with controllable machine parameters.

## 2 Planning of Experiments

The strength of PLA parts is governed by a large number of interactive variables. In this study three controllable variables have been considered, namely, layer thickness, nozzle diameter, and part bed temperature to carry out experimental work. The experiments were conducted keeping these process parameters at various levels. The parts were fabricated on Protocentre 999 3D printer. On the basis of past literature reviews and capabilities of 3D printing machine, the range for each of the process parameter was selected. The range for nozzle diameter was selected from 0.3 to 0.5 mm, layer thickness 0.1 to 0.3 mm, and the part bed temperature from 51 to 53 °C respectively. The range of process parameters have been given in Table 1. The physical properties of PLA have been provided in Table 2. In this study, single variable experiments have been carried out.

**Table 1** Range of process parameters

Parameters	Range
Layer thickness (mm)	0.1, 0.2, 0.3
Nozzle diameter (mm)	0.3, 0.4, 0.5
Part Bed temperature (°C)	51, 53, 55
Raster orientation (°)	45°/-45°
Extruder head speed	100 mm/sec
Temperature of extruder (°C)	220

**Table 2** Physical properties of solidified PLA [12]

Parameters	Value
Grade	4043D
Density (g/cm <sup>3</sup> )	1.24
Glass Transition Temperature (°C)	60
Melting point (°C)	160

**Fig. 1** Specimen fabricated for tensile test (type 1)

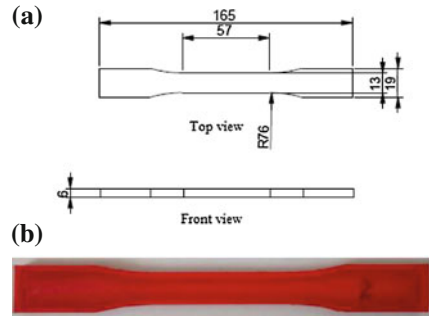
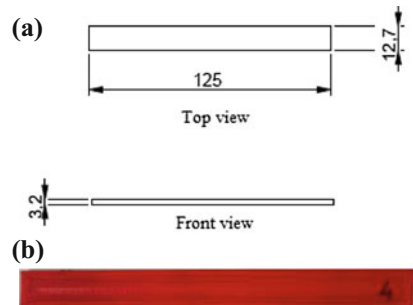


Figure 1 shows the specimen dimensions and specimen fabricated for tensile test. Tensile strength at break is determined on UTE 100 instrument according to ASTM D638 testing standards. Capacity of UTE 100 is 100 KN with minimum resolution of 0.05 KN. Crosshead speed at which testing was done is 5 mm/min. Flexural strength at yield is determined as per ASTM D790-10 shown in Fig. 2, in which three-point bending test is used for flexural strength determination. The specimen is supported by two supports and loaded in the middle by force until the test specimen fractures. Three-point bending test was performed on UTN 20, having capacity of 2000 kgf with minimum resolution of 4 kgf. The crosshead speed during testing was set to 2 mm/min.

**Fig. 2** Specimen fabricated for flexural test



### 3 Results and Discussions

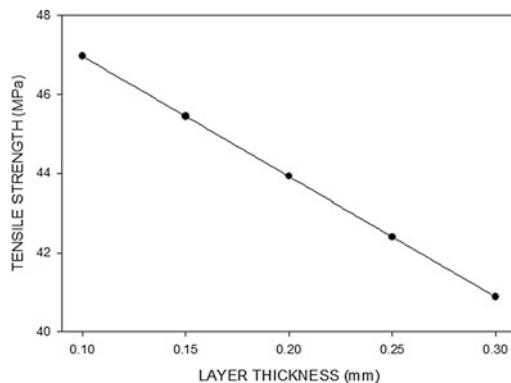
#### 3.1 Analysis for Tensile Strength

From Fig. 3, it can be noted that tensile strength increases as layer thickness decreases. The strong inter layer bonding is one of the important factor for the strength. As the layer thickness decreases, more number of layers will be required [13]. More the number of layers required, higher would be time required to fabricate the part, which will result in more heat dissipation between layers and improve the bond formation between rasters.

During manufacturing of the parts, there is formation of voids between the adjacent layers, which is due to very high scanning speeds. Layer thickness is one of the important factor on which the volume of this voids depends. Figure 4 shows the scanning electron microscope (SEM) images for the 0.1 and 0.2 mm layer thickness. It is visible from Fig. 4b that voids dimensions are lower in 0.1 mm layer thickness as compared to the 0.2 mm layer thickness (Fig. 4a). Larger the void dimension, poor the inter layer bonding between layers will take place. Due to lower layer thickness, total volume of the voids taking place between the layers is minimum as compared to the higher layer thickness. Small air gap helps to provide strong bond between rasters and thus, improves strength.

Figure 5 shows that tensile strength increases as part bed temperature increases. Increase in part bed temperature provides strong inter-layer bonding. As the part bed temperature increases, there is increase in heat dissipation from one layer to another, which leads to post heating of layers which are already bonded. Due to this post heating of layers, greater diffusion of one layer to the adjacent layer occurs and hence improves the strength. On additional experimentation, when we approached the glass transition temperature, it was observed that the tensile strength started to decrease. The effective range of temperature where tensile strength increased was from 51 to 58 °C.

**Fig. 3** Variation of tensile strength with layer thickness



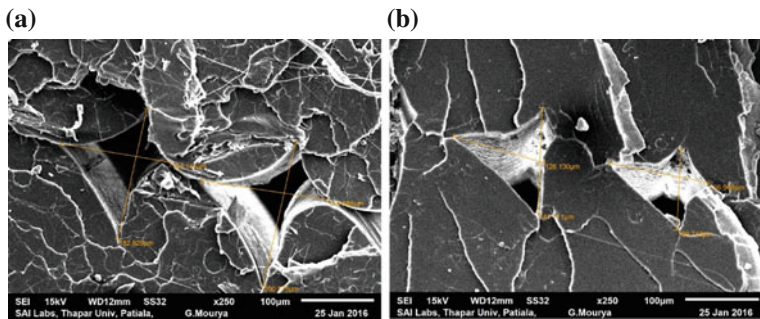


**Fig. 4** SEM image of tensile failure of part, **a** void dimensions for 0.2 mm layer thickness, **b** void dimensions for 0.1 mm layer thickness

**Fig. 5** Variation of tensile strength with part bed temperature

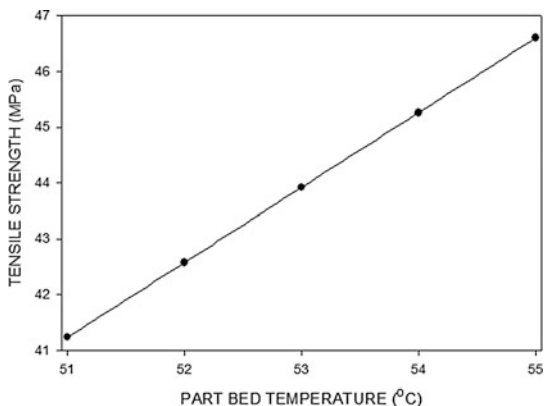


**Fig. 6** Variation of tensile strength with nozzle diameter

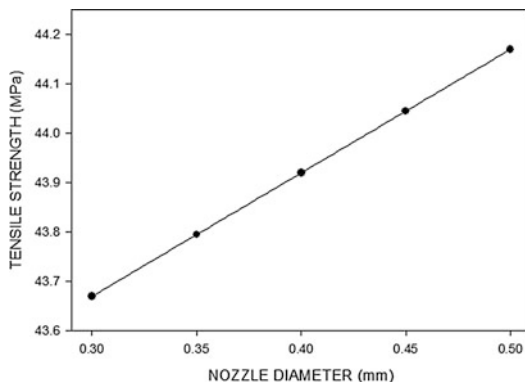
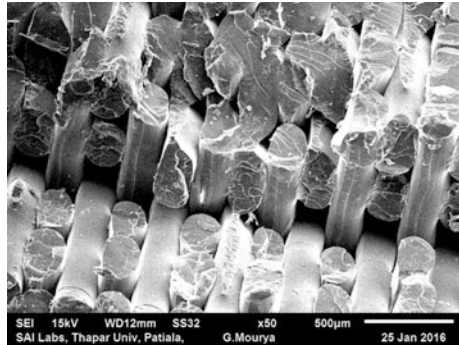


Figure 6 shows that there is an increase in tensile strength with increase in nozzle diameter. As the nozzle diameter increases, the width of the layer also increases. This provides more width for successive layers to bind, resulting in an increase in the

**Fig. 7** SEM image of tensile specimen showing the rupture of fibres



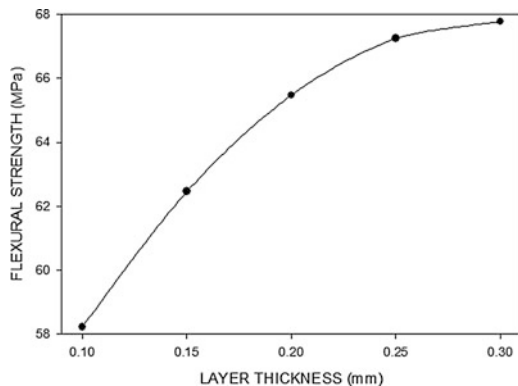
tensile strength. But the increase in strength is very less hence it is not a significant factor for tensile strength.

Figure 7 shows the SEM image of fractured surface. It can be clearly observed that failure has been caused because of rupturing due to pulling of fibres and rasters. It can be further observed that the material breakage of raster occurs in a plane approximately normal to a tensile stress.

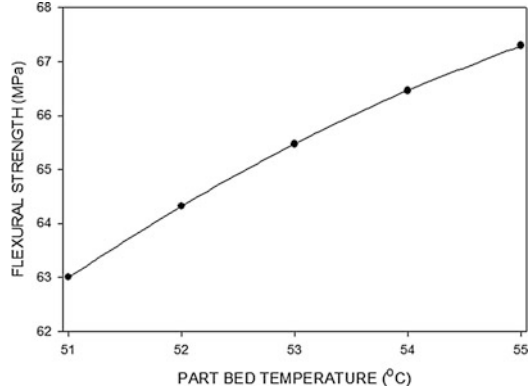
### 3.2 Analysis for Flexural Strength

From Fig. 8, it can be observed that flexural strength of the part increases as the layer thickness increases. In flexural testing of the parts, the direction of force is normal to the direction of layers. Here raster orientation is  $45^{\circ}$ – $45^{\circ}$  in all the parts which are fabricated. In case of flexural testing of the part, strength increases with the increase of raster angle and layer thickness. In flexural testing the top surface layers of the part will observe compressive stress and lower surface layers will observe tensile stress. The layer bonding of tensile stress side layer is slightly strong

**Fig. 8** Variation of flexural Strength with layer thickness



**Fig. 9** Variation of flexural strength with part bed temperature

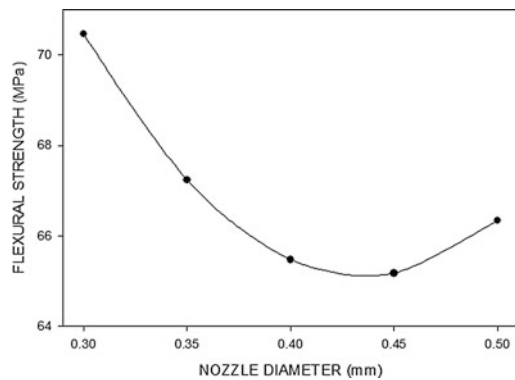


because of high temperature gradient from bottom to top layers. Due to increase in layer thickness with higher raster angle, reduction in the distortion of the layers because elevated raster angles generate smaller rasters which are difficult to bend [14].

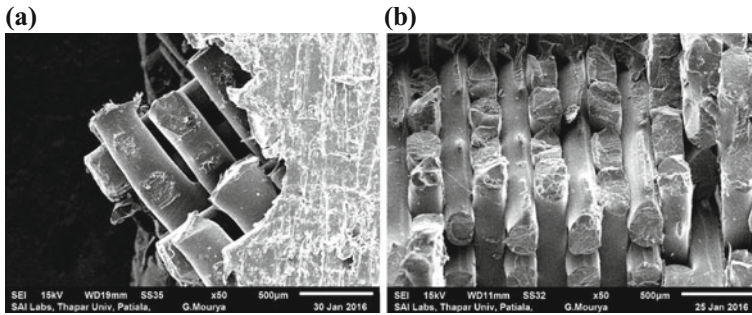
Figure 9 shows the consequence of part bed temperature on the flexural strength of the part. It can be observed that flexural strength of the part increases with increase in part bed temperature. The reason for increase in strength is same as in case of tensile strength, which is the increase in heat dissipation from one layer to another. This leads to post heating of layers which are already bonded and results in improved strength.

Figure 10 shows the outcome of nozzle diameter on the flexural strength of the part. It shows that flexural strength decreases with increase in nozzle diameter firstly and then increases with increase in nozzle diameter. This may be because as the nozzle diameter initially increased, there were large voids observed between the successive layering, which despite more surface contact area, results in inferior strength. At larger nozzle diameter, these voids decreased in dimensions hence the increase in flexural strength.

**Fig. 10** Variation of flexural strength with nozzle diameter







**Fig. 11** SEM image of flexural specimen **a** side view, **b** top view

Fracture behavior of flexural specimen reveals that failure starts at the bottom side of the part, that is, the tensile side of the specimen which is shown in Fig. 11. However the pieces are seized together by non fragmented fibres of top side and the crack propagation in the direction of load is nearly straight. Compression side that is the top side of the specimen breaks by bending of the fibres. It can be further observed that the failure is caused because of tearing and breaking of rasters and material.

## 4 Conclusions

The relationship for layer thickness, part bed temperature, and nozzle diameter with respect to tensile strength and flexural strength for PLA has been analyzed in this paper. It has been observed that as the layer thickness increases, tensile strength decreased where as flexural strength increased. As the part bed temperature increased, tensile strength and flexural strength also increased. With respect to nozzle diameter, tensile strength increased while flexural strength initially decreased and then increased with increase in nozzle diameter. The failure in tensile testing has been caused because of rupturing due to pulling of fibres. Fracture behavior of flexural specimen reveals that failure starts at the bottom side of the part of the specimen.

## References

1. D.T. Pham, S.S. Dimov, *Rapid Manufacturing. The Technologies and Applications of Rapid Prototyping and Rapid Tooling* (Springer, London, 2001)
2. S.H. Ahn, M. Montero, D. Odell, S. Roundy, P.K. Wright, Anisotropic material properties of fused deposition modeling ABS. *Rapid Prototyp. J.* **8**(4), 248–257 (2002)

3. D. Karalekas, K. Antoniou, Composite rapid prototyping: overcoming the drawback of poor mechanical properties. *J. Mat. Process. Tech.* **153–154**, 526–530 (2004)
4. K.C. Ang, K.F. Leong, C.K. Chua, Investigation of the mechanical properties and porosity relationships in fused deposition modelling-fabricated porous structures. *Rapid Prototyp. J.* **12**(2), 100–105 (2006)
5. P.K. Jain, P.M. Pandey, P.V.M. Rao, Effect of delay time on part strength in selective laser sintering. *Int. J. Adv. Manuf. Tech.* **43**, 117–126 (2009)
6. A. Bagsik, V. Schoeppner, E. Klemp, FDM part quality manufactured with Ultem\* 9085, in *Proceedings 14th International Scientific Conference on Polymeric Materials 2010*, Halle (Saale) (2010)
7. G. Percoco, F. Lavecchia, L.M. Galantucci, Compressive properties of FDM rapid prototypes treated with a low cost chemical finishing. *Res. J. Appl. Sci. Engg. Tech.* **4**(19), 3838–3842 (2012)
8. D. Croccolo, M. De Agostinis, G. Olmi, Experimental characterization and analytical modelling of the mechanical behaviour of fused deposition processed parts made of ABS-M30. *Comput. Mater. Sci.* **79**, 506–518 (2013)
9. B.M. Tymrak, M. Kreiger, J.M. Pearce, Mechanical properties of components fabricated with open-source 3-D printers under realistic environmental conditions. *Mater. Des.* **58**, 242–246 (2014)
10. F. Afrose, S.H. Masood, P. Iovenitti, M. Nikzad, I. Sbarski, Effects of part build orientations on fatigue behavior of FDM-processed PLA material. *Prog. Addit. Manuf.* <https://doi.org/10.1007/s40964-015-0002-3>
11. D.A. Roberson, A.R.T. Perez, C.M. Shemelya, A. Rivera, E. MacDonald, R.B. Wicker, Comparison of stress concentrator fabrication for 3D printed polymeric izod impact test specimens. *Addit. Manuf.* **7**, 1–11 (2015)
12. <http://www.natureworksllc.com>, TechnicalDataSheet \_ 4043D \_ 3D -monofilament\_pdf
13. A.K. Sood, R.K. Ohdar, S.S. Mahapatra, Parametric appraisal of mechanical property of fused deposition modelling processed parts. *Mater. Des.* **31**, 287–295 (2010)
14. H. Persson, K. Adan, “Modeling and experimental studies of PC/ABS at large deformations,” Master’s Thesis, Division of Solid Mechanics, Lund University, Lund, Sweden, (2004)